Published in final edited form as:
NMR Biomed. 2014 August ; 27(8): 996–1004. doi:10.1002/nbm.3143.

Arterial Spin Labeling - Fast Imaging with Steady-State Free Precession (ASL-FISP): A Rapid and Quantitative Perfusion Technique for High Field MRI

Ying Gao[1,2,†], **Candida L. Goodnough**[3,†], **Bernadette O. Erokwu**[1], **George W. Farr**[3,4], **Rebecca Darrah**[5,6], **Lan Lu**[1,7], **Katherine M. Dell**[8,9], **Xin Yu**[1,2,3], and **Chris A. Flask**[1,2,9]

[1]Department of Radiology, Case Western Reserve University, Cleveland, OH 44106.

[2]Department of Biomedical Engineering, Case Western Reserve University, Cleveland, OH 44106.

[3]Department of Physiology and Biophysics, Case Western Reserve University, Cleveland, OH 44106.

[4]Aeromics, LLC, Cleveland, OH 44106.

[5]Frances Payne Bolton School of Nursing, Case Western Reserve University, Cleveland, OH 44106.

[6]Department of Genetics and Genome Sciences, Case Western Reserve University, Cleveland, OH 44106.

[7]Department of Urology, Case Western Reserve University, Cleveland, OH 44106.

[8]CWRU Center for the Study of Kidney Disease and Biology, MetroHealth Campus, Case Western Reserve University, Cleveland, OH 44109.

[9]Department of Pediatrics, Case Western Reserve University, Cleveland, OH 44106.

Abstract

Arterial Spin Labeling (ASL) is a valuable non-contrast perfusion MRI technique with numerous clinical applications. Many previous ASL MRI studies have utilized either Echo-Planar Imaging (EPI) or True Fast Imaging with Steady-State Free Precession (True FISP) readouts that are prone to off-resonance artifacts on high field MRI scanners. We have developed a rapid ASL-FISP MRI acquisition for high field preclinical MRI scanners providing perfusion-weighted images with little or no artifacts in less than 2 seconds. In this initial implementation, a FAIR (Flow-Sensitive Alternating Inversion Recovery) ASL preparation was combined with a rapid, centrically-encoded FISP readout. Validation studies on healthy C57/BL6 mice provided consistent estimation of *in vivo* mouse brain perfusion at 7 T and 9.4 T (249±38 ml/min/100g and 241±17 ml/min/100g, respectively). The utility of this method was further demonstrated in detecting significant perfusion deficits in a C57/BL6 mouse model of ischemic stroke. Reasonable kidney perfusion

Corresponding author: Chris A. Flask, Ph.D., Assistant Professor of Radiology, Biomedical Engineering, and Pediatrics, Case Western Reserve University, University Hospitals of Cleveland, 11100 Euclid Avenue, Bolwell Building, Room B115, Cleveland, OH 44106, PH: 216-844-4963, Fax: 216-844-4987, caf@case.edu.
[†]These authors contributed equally to this work.

estimates were also obtained for a healthy C57/BL6 mouse exhibiting differential perfusion in the renal cortex and medulla. Overall, the ASL-FISP technique provides a rapid and quantitative *in vivo* assessment of tissue perfusion for high field MRI scanners with minimal image artifacts.

Keywords

perfusion; high field MRI; FISP; arterial spin labeling

INTRODUCTION

Arterial Spin Labeling (ASL) MRI is a non-contrast perfusion MRI technique that has been shown to provide quantitative assessments of tissue perfusion in multiple clinical imaging applications including brain (1–3), kidney (4–7), lung (8–12), and liver (13). One major advantage of ASL over conventional Dynamic Contrast Enhanced MRI perfusion techniques is the lack of exogenous, and potentially toxic, paramagnetic contrast agents. The use of endogenous blood signal to obtain tissue perfusion information is especially important for imaging patients with chronic kidney diseases, which can be a contraindication for Gadolinium-based MRI perfusion methods (14). This attribute is also important for longitudinal preclinical imaging applications, as multiple tail-vein injections and/or catheterizations can cause local inflammation and necrosis resulting in reduced access to veins.

ASL MRI techniques generate blood flow contrast between multiple images using a wide variety of blood labeling methods (15–20). A typical ASL MRI acquisition combines an ASL preparation phase followed by a rapid imaging readout to capture the blood flow–weighted contrast (Figure 1). It is important to note that a large majority of the imaging developments have focused on optimization of the preparation phase of the ASL acquisition. As a result, a wide variety of preclinical and clinical ASL MRI techniques have been developed. These ASL techniques can be broadly grouped into continuous (CASL, (15,16,20)) and pulsed (PASL, (17–19)) categories. A hybrid of these two techniques, pseudo-continuous ASL (pCASL) has also been recently developed (21–23). Each of these specialized techniques offers advantages for specific imaging applications. At the same time, many of these studies have utilized conventional imaging readouts including Fast Low Angle SHot (FLASH) (24,25), Echo-Planar Imaging (EPI) (26,27), and True Fast Imaging with Steady-State Free Precession (True FISP) (5,12,28,29). Unfortunately, these imaging readouts exhibit significant limitations for high field MRI applications. Specifically, B_0 inhomogeneities result in increased distortion / ghosting and banding artifacts from EPI and True FISP imaging techniques, respectively on high field MRI scanners. These artifacts are particularly problematic for body imaging applications where cardiac and respiratory motion as well as adipose tissue can make precise shimming difficult. In addition, the increase in T_1 magnetic relaxation times on high field MRI scanners can result in spoiled gradient echo images with a lower signal-to-noise ratio (SNR) relative to these other imaging techniques. A lower SNR is especially problematic for ASL MRI techniques as the differential blood flow signal is typically less than 10% of the mean tissue signal (30,31). Therefore, a need exists to develop a rapid and robust ASL MRI imaging readout that is both sensitive to

blood flow labeling from the ASL preparation and also immune to B_0 inhomogeneities and motion artifacts on high field MRI scanners.

Our group has previously reported on the development of a centrically-encoded FISP imaging technique which can be flexibly combined with conventional diffusion and magnetization transfer (MT) / chemical exchange saturation transfer (CEST) preparation methods to rapidly generate quantitative imaging data (32,33). Importantly, the magnetic field gradients for the FISP readout sequence are not completely refocused in either the slice select or frequency encoding directions, resulting in greatly reduced off-resonance artifacts in comparison to EPI and True FISP acquisitions. In addition, centric k-space encoding of the FISP readout retains the image contrast generated in the diffusion and MT / CEST preparations.

Here, we describe initial *in vivo* results from an ASL-FISP acquisition on 7T and 9.4T Bruker Biospec small animal MRI scanners. For this initial study, our ASL-FISP implementation combines a FAIR preparation scheme with our rapid centrically-encoded FISP imaging readout to generate ASL imaging data (5,19,29,34). The reproducibility of this new ASL-FISP technique was evaluated in brains of healthy C57/BL6 mice. In addition, we demonstrate the effectiveness of this technique for multiple imaging applications including mouse models of ischemic stroke and healthy mouse kidneys.

METHODS

In Vivo Comparison of Image Artifacts at 7T

Axial FISP images of a healthy C57/BL6 mouse brain were acquired on a 7 T Bruker Biospec MRI scanner (Bruker Inc., Billerica, MA) for comparison to conventional spin echo (TR/TE = 2000/14 ms, 1 average, total scan time = 4 min 16 s), True FISP (TR/TE = 4.0/2.0 ms, 20 averages, tip angle = 60 degrees, total scan time = 11 s), and EPI (TR/TE = 2500/30.8 ms, 4 segments, 2 averages, total scan time = 20 s) imaging readout methods to assess image artifacts.

ASL-FISP pulse sequence design

The ASL-FISP acquisition was implemented on Bruker Biospec 7 T and 9.4 T MRI scanners equipped with 400 mT/m gradient inserts. The ASL-FISP sequence was implemented on both MRI scanners to demonstrate the robustness of the methodology to artifacts on high field MRI scanners. The ASL-FISP pulse sequence was developed by combining a FAIR preparation (slice-selective or non-selective inversion) with a centrically-encoded FISP imaging readout to acquire all lines of k-space following each ASL preparation (Figure 1). Note that although a FAIR scheme was implemented herein, the ASL-FISP technique is adaptable to a variety of ASL preparations. A hermite excitation RF pulse of duration 0.5 ms, and a tip angle of 60 degrees was the selected for this implementation. The high tip angle was selected for this FISP acquisition to provide increased SNR in comparison to low tip angles (data not shown).

Uniformity of the inversion pulse is essential for accurate and precise quantification of tissue perfusion. Therefore, a hyperbolic secant adiabatic inversion pulse of duration 3.0 ms was

used for the FAIR inversion preparation. Magnetic field gradient spoilers were applied after the inversion preparation to limit transverse magnetization prior to the FISP imaging readout. The FISP imaging readout (including 10 dummy scans) provided *in vivo* images in less than 2 seconds with relatively high SNR in comparison to conventional spoiled gradient echo acquisitions and minimal off-resonance distortion and ghosting artifacts in comparison to EPI (32,33). The FISP imaging readout also prevented banding artifacts typical of balanced SSFP / True FISP acquisitions on high field MRI scanners. The FISP imaging readout was also designed with centric encoding to retain blood flow sensitivity as well as the T_1 weighting generated from the FAIR inversion preparation.

Initial *in vivo* ASL-FISP perfusion assessments in mouse brains

All animal studies were conducted in accordance with approved IACUC (Institutional Animal Care and Use Committee) protocols at Case Western Reserve University. The ASL-FISP technique was initially evaluated by assessing brain perfusion in healthy wild-type C57/BL6 mice (The Jackson Laboratory, Bar Harbor, Maine). Each animal was anesthetized in 1–2% isoflurane with supplemented O_2 and positioned within a mouse volume coil (inner diameter = 35mm) in a Bruker Biospec MRI scanner (Bruker Inc., Billerica, MA). Each animal's body temperature was maintained at 35±1 °C with a warmed air control system. Respiratory triggering was performed through an MR-compatible small animal gating and control system (SA Instruments, Stony Brook, NY).

Ten male C57/BL6 10 weeks of age were scanned with the ASL-FISP imaging protocol at 7 T. Five of these mice were scanned with the ASL-FISP imaging protocol at 9.4 T at least one day prior to the 7 T scan for comparison. Rapid localizer scans were first used to identify an appropriate and consistent axial mid-brain imaging slice for the ASL-FISP protocol. After slice positioning, the single-slice ASL-FISP protocol consisted of three sequential scans: 1) ASL-FISP with a slice-selective inversion, 2) ASL-FISP with non-selective inversion, and 3) FISP with no inversion preparation as a reference (M0) scan for blood flow calculation (19). An inversion delay time (TI) of 1420 ms was used for this initial implementation to generate sufficient blood flow contrast between the slice-selective and non-selective ASL-FISP images. Other than the inversion preparation, the FISP imaging readout parameters were identical among these three acquisitions (centric encoding, TR/TE = 2.4/1.2 ms, matrix = 128 × 128, FOV = 3 cm × 3 cm, imaging slice thickness = 1.5 mm, tip angle = 60 degrees). These scans were repeated 60 times to determine the effects of image quality on the perfusion calculations. Although not required, for this initial implementation an additional delay time of ~13 seconds was incorporated between each scan repetition to allow the magnetization to return to equilibrium (M_0) between repetitions and to limit the duty cycle on the magnetic field gradients. The total acquisition time for one ASL-FISP repetition including the ASL preparation (1420 ms), FISP imaging readout (331 ms), and ~13-second delay was 15 seconds.

For comparison, we also implemented an ASL-GRE acquisition by combining an identical FAIR preparation with a gradient echo (GRE) imaging readout (TR/TE = 5000/2 ms, 5 averages, tip angle = 90 degrees). For this simplified ASL-GRE acquisition, only one line of k-space was acquired for each ASL preparation. All other imaging parameters including

field of view (FOV) and resolution were identical to the ASL-FISP acquisitions described above. This conventional ASL-GRE acquisition was evaluated on a separate single healthy C57/BL6 mouse brain at 7 T for direct comparison with the ASL-FISP results.

Following the ASL-FISP scans, a FISP-based Look-Locker acquisition was then implemented to generate voxel-wise T_1 maps according to previously described techniques (35,36). The Look-Locker acquisition consisted of a non-selective adiabatic inversion followed by 10 continuous and sequential FISP image repetitions (linear encoding, tip angle = 10 degrees, TR/TE = 4.0 ms / 2.0 ms, 512 ms / image). The Look-Locker acquisition was repeated at least 40 times to ensure accurate T_1 relaxation time estimation. As for the ASL-FISP acquisitions above, a ~7-second delay was introduced after each repetition to reduce the duty cycle on the imaging gradients and to allow the magnetization to return to equilibrium (M_0). Voxel-wise T_1 relaxation maps were then calculated according to previously described methods (35,36). The geometry of the Look-Locker acquisition was identical to the ASL-FISP acquisitions to ensure one-to-one correspondence between the ASL and T_1 relaxation data and enable direct calculation of the quantitative ASL maps described below.

Quantitative, voxel-wise perfusion maps were generated using previously described methods for the FAIR ASL technique according to Equation 1 below (18,19).

$$f=\frac{\lambda}{2TI}\frac{SS(TI)-NS(TI)}{M0}\exp\left(\frac{TI}{T_1}\right) \quad [1]$$

where f is the tissue perfusion in ml/min/100g of tissue; NS, SS, and M0 are the signal intensities for the non-selective, slice-selective, and reference (M0) ASL-FISP images, respectively; T_1 is the longitudinal relaxation time calculated from the Look-Locker acquisition; TI is the inversion time set at 1420 ms; and the tissue-blood partition coefficient (λ) was assumed to be 0.9 ml/g (37). Perfusion maps were calculated using this equation for each ASL-FISP scan.

A region-of-interest (ROI) analysis was then used to calculate the mean perfusion over the entire mouse brain visible within the single ASL-FISP imaging slice. Note that these ROIs included both white matter and gray matter, while ventricles were excluded from the analysis. A histogram analysis of the mouse brain ROI was also used to calculate a threshold (mean ± 2 standard deviations) to limit the impact of large vessels (high perfusion values) on the calculation of the mean brain perfusion value for each animal similar to previously described methods (3,5). The mean brain perfusion values for each individual mouse were then used to calculate an overall group average and standard deviation at 7 T and 9.4 T respectively, for comparison. This ROI analysis was repeated for 20, 40, and 60 ASL-FISP averages at 7 T and 9.4 T to perform an initial determination of the effects of noise on the brain perfusion assessments. For all C57/BL6 mice, ASL-FISP scans were obtained with an inversion slab thickness three times that of the FISP imaging slice thickness to ensure a uniform inversion over the entire FISP imaging slice. This factor of three was previously described by our group (32) and provides an effective balance between blood flow sensitivity and inversion uniformity. One C57/BL6 mouse was scanned with an inversion

slab thickness / imaging slice thickness ratio of 1, 3, 6, and 10 to determine the effects of the relative inversion slab thickness on the perfusion results.

Additional *in vivo* ASL-FISP experiments: mouse brain ischemic stroke model and healthy mouse kidneys

The ASL-FISP acquisition and analysis protocol described above was performed on two additional C57/BL6 mice to evaluate: (1) brain perfusion in the context of known pathology (ischemic stroke); (2) kidney perfusion; and (3) muscle perfusion. Except for the number of signal averages (40), all of the imaging parameters used for these imaging studies were identical to the brain ASL-FISP experiments described above.

An ASL-FISP study was performed on a mouse model of ischemic stroke to assess the method's sensitivity to a known pathophysiology. A C57/BL6 mouse (male, 8 weeks of age), was anesthetized with isoflurane. A transient stroke was initiated by inserting a 0.22 mm diameter, silicon-coated filament (Doccol, Corp) into the right carotid artery resulting in an occlusion of the middle cerebral artery (MCAo), while monitoring cerebral blood flow using Laser Doppler flowmetry (38–40). The filament was removed after one hour of occlusion to allow reperfusion as the animal recovered. At 24 hours post-*ictus*, the animal was re-anesthetized for ASL-FISP scanning as described above. A diffusion weighted EPI image (TR/TE = 5000 / 31 ms, b=500 s/mm^2) was also acquired to confirm the presence of the infarct from the MCAo. A brain perfusion map and a mean perfusion value for the whole brain within the imaging slice were calculated for comparison with healthy C57/BL6 mice.

For the kidney and paraspinal muscle perfusion assessment, ASL-FISP was performed on a healthy male 10-week-old C57/BL6 mouse. Respiratory triggering was performed as described above. This study was performed as an initial demonstration of the effectiveness for ASL-FISP for high field body imaging applications. Following the ASL-FISP acquisitions, an ROI analysis was used to calculate the mean renal perfusion values for the left and right kidneys of this mouse and the mean perfusion value of the paraspinal muscles.

RESULTS

Axial mouse brain images from spin echo, FISP, True FISP and EPI imaging techniques at 7 T are shown in Figure 2. Banding and ghosting / distortion artifacts are clearly visible in the True FISP and EPI images, respectively. By comparison, the spin echo and FISP images show a lack of image artifacts with the FISP images generated in less than 1/10th of the acquisition time (22 seconds vs 4 minutes 16 seconds). Representative brain ASL-FISP image sets, T_1 relaxation time maps, and calculated perfusion maps are shown for a healthy C57/BL6 mouse at 7 T (n=10) in Figure 3. Qualitatively similar images and maps were obtained from the mice at 9.4 T (n=5, data not shown). The mean and standard deviations for the groups of healthy mice scanned at 7 T and 9.4 T are shown in Figure 4a as a function of the number of ASL-FISP averages used to calculate the perfusion data (20, 40, and 60 averages). A 2-tailed Student's t-test showed no significant difference between the mean perfusion values at the two magnetic field strengths ($p > 0.2$) or for 20, 40, and 60 averages ($p > 0.6$). With 40 signal averages, the mean brain perfusion values for healthy C57/BL6 mice ranged from 210 – 333 ml/min/100g of tissue at 7 T and 222 – 268 ml/min/100g of

tissue at 9.4 T, respectively. The mean ± standard deviation of the mouse brain perfusion (excluding ventricles) at 7 T and 9.4 T were 249 ± 38 ml/min/100g of tissue and 241 ± 17 ml/min/100g of tissue, respectively.

A secondary ROI analysis of the 7T mouse brain perfusion data showed differential perfusion values in the cortex (211 ± 30 ml/min/100g) and thalamus (288 ± 48 ml/min/100g), which is consistent with previous studies (41). A perfusion map from the ASL-GRE method (mean cerebral perfusion = 285 ml/min/100g) is shown in Figure 3f for comparison. The total imaging time for 5 averages was approximately 4 hours. In order to make a valid comparison between protocols, the time under anesthesia should be consistent to ensure similar perfusion conditions. We chose to evaluate the ASL-GRE method with 2 averages so that the imaging time was approximately the same as ASL-FISP. The mean cerebral perfusion value from the ASL-FISP method (40 averages) was 249 ± 38 ml/min/100g, which is quite reasonable compared to the cerebral perfusion value of 240 ml/min/100g from the ASL-GRE method (2 averages).

The mean brain perfusion values from a single C57/BL6 mouse using an inversion slab thickness / imaging slice thickness ratio of 1, 3, 6, and 10 and either 5, 10, 20, 40, or 60 ASL-FISP averages are shown in Figure 4b. A large decrease in perfusion was observed as the inversion slab thickness / imaging slice thickness ratio was increased from 1 (inversion slab thickness = imaging slice thickness) to 3 due to both increased uniformity of the inversion pulse over the entire imaging slice and reduced perfusion sensitivity. The mean brain perfusion values continued to decrease at a lower rate as the inversion slab thickness / imaging slice thickness ratio increase from 3 to 6 and 10. In addition, only minimal variation was observed in the mean perfusion values as the number of ASL-FISP is reduced from 60 to 5 for each ratio.

Axial ASL images, T_1 maps, and brain perfusion maps for the middle cerebral artery occlusion (MCAo) model of ischemic stroke in a mouse are shown in Figure 5. The region of infarct on the right side of the brain (left side of image) is clearly visible in the ASL-FISP images and the corresponding perfusion map. Note that a smaller secondary infarct is visible on the contralateral side most likely resulting from the extensive cytotoxic edema caused by the induced ischemic stroke. Overall, the mean brain perfusion for the MCAo mouse was measured to be 143 ml/min/100g.

Axial ASL images, T_1 maps, and perfusion maps for the C57/BL6 mouse kidneys are shown in Figure 6. As expected, the aorta and renal arteries show a very bright signal in the slice-selective inversion ASL-FISP image (Figure 6a), while the arterial blood signal is greatly attenuated for the non-selective ASL-FISP image (Figure 6b). The measured mean renal perfusion values for the left and right kidneys (cortex + medulla + pelvis) were 513 and 560 ml/min/100g, respectively. In addition, the perfusion in the renal cortex was visibly increased relative to the renal medulla as expected. Importantly, mouse kidney perfusion was approximately twice that of the brain perfusion, consistent with previous reports (23,27,42,43). The mean perfusion value in the paraspinal muscles was 81 ml/min/100g, which was significantly lower than that of the kidneys as expected (23).

DISCUSSION

In this study, initial *in vivo* ASL MRI results were obtained using a rapid and artifact-resistant ASL-FISP acquisition on 7 T and 9.4 T small animal MRI scanners. The ASL-FISP technique combines an inversion preparation (slice-selective or non-selective) followed by a centrically-encoded FISP imaging readout to provide ASL data with minimal image artifacts in comparison to conventional EPI and True FISP imaging readouts for ASL MRI acquisitions.

There are several important design features of the ASL-FISP acquisition. Most importantly, the FISP imaging readout is applied with centric k-space encoding and relatively few (i.e., 10) dummy scans. As shown previously, this centric encoding approach minimizes the loss of perfusion sensitivity caused by additional radiofrequency pulses and gradient lobes encountered in linear k-space encoding (33). A FISP imaging readout was selected for this study instead of a balanced SSFP readout primarily to limit well-known banding artifacts that are significantly increased on high field MRI scanners. An alternative approach using balanced SSFP would be to acquire multiple images with different RF phase variation sequences to reconstruct banding free image (44,45). This approach may offer increased signal-to-noise, but it may require additional image processing to remove the banding artifacts. As a result, this alternative approach and direct comparison with ASL-FISP was not explored for this initial study. Further studies are also needed to directly compare the FISP and True FISP techniques as the FISP flow sensitivity may be altered due to dephasing (46).

Overall, the key advantage of the FISP imaging readout is that it provides perfusion sensitivity with a short acquisition time (~2 seconds / image) with minimal artifacts in comparison to EPI readouts. The ASL-FISP and ASL-GRE acquisitions generated relatively similar perfusion maps (Figure 3) and mean brain perfusion values. However, the ASL-GRE method required an acquisition time that was more than 50 times than that of the ASL-FISP method. In addition, the FISP imaging readout can easily be coupled with virtually any ASL preparation in order to meet the requirements for specific imaging applications. For this initial implementation, a simple FAIR ASL preparation was implemented with either a slice-selective or non-selective inversion pulse. However, more complex ASL preparations such as pCASL could also be implemented in order to measure transit times and other important perfusion parameters (23). The FISP imaging readout is particularly relevant for FAIR acquisitions as the difference between the images with the slice-selective inversion and non-selective inversion is small relative to the M0 image (typically < 10%). As a result, FAIR-ASL studies generally require numerous signal averages to obtain a reasonable estimate of tissue perfusion. Therefore, acquiring all k-space lines following a single ASL preparation (with minimal artifacts) using the FISP readout results in practical imaging times to acquire sufficient signal averages. While only single slice ASL-FISP results are presented in this initial study, multi-slice and/or 3D ASL-FISP implementations are possible and may have significant advantages for specific imaging applications.

Initial *in vivo* mouse brain perfusion studies demonstrated that the ASL-FISP technique provides reasonable perfusion assessments on high field MRI scanners. ASL-FISP images in

the healthy mouse brain and an induced ischemic stroke model show an expected lack of distortion and artifacts and clearly delineated perfusion deficits in the stroke model (Figures 3 and 5, respectively). Further, the kidney ASL-FISP images and perfusion maps in Figure 6 show differential perfusion between the renal cortex and medulla as expected from prior studies (5,47). In addition, the renal arteries are clearly visible in both the slice-selective inversion ASL-FISP images as well as the perfusion maps demonstrating the flow sensitivity of the ASL-FISP technique. Overall, the reliability of the ASL-FISP technique is exhibited by the lack of differences in the perfusion results at 7 T and 9.4 T (Figure 4a). Most importantly, the mouse kidney images shown in Figure 6 demonstrate that the ASL-FISP technique can provide high quality ASL data for rodent brain and body imaging applications on high field MRI scanners with no distortion and artifacts.

The ASL-FISP technique presented herein also has several important limitations. One key observation of these initial results is that the mean perfusion values for mouse brains and kidneys shown here are dependent on the perfusion preparation scheme and inversion pulse design. It has already been shown in multiple studies that the relative thickness between the slice-selective inversion and the imaging readout is directly related to the resulting tissue perfusion estimate (2,4,28,31). For example, a smaller inversion slab thickness (ex. 1× that of the imaging slice) will result in enhanced perfusion sensitivity and erroneously high perfusion estimates. Conversely, a larger inversion slab thickness (ex. 6 × that of the imaging slice) will result in reduced perfusion sensitivity. These results are reflected in Figure 4b which shows that an inversion slab thickness / imaging slice ratio ≥ 3 is needed to maintain reasonably consistent perfusion results. The perfusion results can also be directly impacted by the shape of the inversion pulse and the excitation pulses of the FISP imaging readout. However, optimization of these pulses was beyond the scope of this initial technical development. Nevertheless, the results shown herein confirm that the ASL-FISP technique can sensitively differentiate normal tissue perfusion from pathology (ex. ischemic stroke) and relative tissue perfusion levels (renal cortex vs. renal medulla vs. skeletal muscle). It is important to note that the ASL-FISP technique may also be sensitive to the effects of pulsatility which may be an underlying cause of the bright CSF signal in the mouse brains.

Another observation of these initial ASL-FISP results is the trend towards lower perfusion values at 9.4 T. While not statistically significant, this trend may be due in part to reduced T_2^* relaxation times at 9.4 T. For mouse brain imaging, this reduction in T_2^* can reduce the SNR of the SS, NS, and M0 images, especially in regions near the ear canals. Fortunately, this potential limitation can be partially mitigated using shorter echo times which would reduce the deleterious T_2^* effects at all field strengths. For the FISP acquisition, the reduction in echo time would provide an additional increase in SNR as the repetition time would also be reduced by the same percentage providing an increase in the coherent steady-state magnetization.

In conclusion, this study reports a rapid and quantitative ASL-FISP MRI technique for high field MRI scanners. For this initial study, the ASL-FISP technique combines a FAIR ASL preparation with a rapid, centrically-encoded FISP imaging readout to provide perfusion-weighted images in less than 2 seconds with minimal image distortion, ghosting, and banding artifacts in comparison to EPI and balanced SSFP readouts. Initial *in vivo* ASL-

FISP perfusion results in mouse brains were obtained for healthy and ischemic stroke C57/BL6 mouse brains at 7 T and healthy mouse brains at 9.4 T. As a demonstration of the invulnerability of the ASL-FISP technique to off-resonance artifacts, initial *in vivo* kidney ASL results were also obtained for C57/BL6 mouse at 7 T. This new technique provides an alternative method for many perfusion imaging applications on high field MRI scanners where off-resonance artifacts can severely limit the use of EPI and balanced SSFP acquisitions.

Acknowledgments

The authors would like to acknowledge the support of NIH/NIDDK RO1 DK085099-01, the Case Comprehensive Cancer Center (P30 CA43703), and the Cystic Fibrosis Foundation.

Abbreviations used

ASL-FISP	arterial spin labeling - fast imaging with steady-state free precession
SSFP	steady-state free precession
EPI	echo-planar imaging
True FISP	true fast imaging with steady-state free precession
FAIR	flow-sensitive alternating inversion recovery
CASL	continuous arterial spin labeling
PASL	pulsed arterial spin labeling
pCASL	pseudo-continuous arterial spin labeling
FLASH	fast low angle shot
SNR	signal-to-noise ratio
MT	magnetization transfer
CEST	chemical exchange saturation transfer
GRE	gradient echo
ROI	region of interest
MCAo	middle cerebral artery occlusion
CSF	cerebrospinal fluid

REFERENCES

1. Wong EC, Buxton RB, Frank LR. Implementation of quantitative perfusion imaging techniques for functional brain mapping using pulsed arterial spin labeling. NMR Biomed. 1997; 10(4–5):237–249. [PubMed: 9430354]
2. Brookes MJ, Morris PG, Gowland PA, Francis ST. Noninvasive measurement of arterial cerebral blood volume using Look-Locker EPI and arterial spin labeling. Magn Reson Med. 2007; 58(1):41–54. [PubMed: 17659615]
3. Boss A, Martirosian P, Klose U, Nagele T, Claussen CD, Schick F. FAIR-TrueFISP imaging of cerebral perfusion in areas of high magnetic susceptibility differences at 1.5 and 3 Tesla. J Magn Reson Imaging. 2007; 25(5):924–931. [PubMed: 17410577]

4. Karger N, Biederer J, Lusse S, Grimm J, Steffens J, Heller M, Gluer C. Quantitation of renal perfusion using arterial spin labeling with FAIR-UFLARE. Magn Reson Imaging. 2000; 18(6):641–647. [PubMed: 10930773]
5. Martirosian P, Klose U, Mader I, Schick F. FAIR true-FISP perfusion imaging of the kidneys. Magn Reson Med. 2004; 51(2):353–361. [PubMed: 14755661]
6. De Bazelaire C, Rofsky NM, Duhamel G, Michaelson MD, George D, Alsop DC. Arterial spin labeling blood flow magnetic resonance imaging for the characterization of metastatic renal cell carcinoma(1). Acad Radiol. 2005; 12(3):347–357. [PubMed: 15766695]
7. Fenchel M, Martirosian P, Langanke J, Giersch J, Miller S, Stauder NI, Kramer U, Claussen CD, Schick F. Perfusion MR imaging with FAIR true FISP spin labeling in patients with and without renal artery stenosis: initial experience. Radiology. 2006; 238(3):1013–1021. [PubMed: 16439565]
8. Mai VM, Berr SS. MR perfusion imaging of pulmonary parenchyma using pulsed arterial spin labeling techniques: FAIRER and FAIR. J Magn Reson Imaging. 1999; 9(3):483–487. [PubMed: 10194721]
9. Mai VM, Bankier AA, Prasad PV, Li W, Storey P, Edelman RR, Chen Q. MR ventilation-perfusion imaging of human lung using oxygen-enhanced and arterial spin labeling techniques. J Magn Reson Imaging. 2001; 14(5):574–579. [PubMed: 11747009]
10. Wang T, Schultz G, Hebestreit H, Hebestreit A, Hahn D, Jakob PM. Quantitative perfusion mapping of the human lung using ^{1}H spin labeling. J Magn Reson Imaging. 2003; 18(2):260–265. [PubMed: 12884340]
11. Bolar DS, Levin DL, Hopkins SR, Frank LF, Liu TT, Wong EC, Buxton RB. Quantification of regional pulmonary blood flow using ASL-FAIRER. Magn Reson Med. 2006; 55(6):1308–1317. [PubMed: 16680681]
12. Martirosian P, Boss A, Fenchel M, Deimling M, Schafer J, Claussen CD, Schick F. Quantitative lung perfusion mapping at 0.2 T using FAIR True-FISP MRI. Magn Reson Med. 2006; 55(5): 1065–1074. [PubMed: 16602073]
13. Katada Y, Shukuya T, Kawashima M, Nozaki M, Imai H, Natori T, Tamano M. A comparative study between arterial spin labeling and CT perfusion methods on hepatic portal venous flow. Jpn J Radiol. 2012; 30(10):863–869. [PubMed: 22986750]
14. Kuo PH, Kanal E, Abu-Alfa AK, Cowper SE. Gadolinium-based MR contrast agents and nephrogenic systemic fibrosis. Radiology. 2007; 242(3):647–649. [PubMed: 17213364]
15. Detre JA, Leigh JS, Williams DS, Koretsky AP. Perfusion imaging. Magn Reson Med. 1992; 23(1):37–45. [PubMed: 1734182]
16. Williams DS, Detre JA, Leigh JS, Koretsky AP. Magnetic resonance imaging of perfusion using spin inversion of arterial water. Proc Natl Acad Sci U S A. 1992; 89(1):212–216. [PubMed: 1729691]
17. Edelman RR, Siewert B, Darby DG, Thangaraj V, Nobre AC, Mesulam MM, Warach S. Qualitative mapping of cerebral blood flow and functional localization with echo-planar MR imaging and signal targeting with alternating radio frequency. Radiology. 1994; 192(2):513–520. [PubMed: 8029425]
18. Kwong KK, Chesler DA, Weisskoff RM, Donahue KM, Davis TL, Ostergaard L, Campbell TA, Rosen BR. MR perfusion studies with T1-weighted echo planar imaging. Magn Reson Med. 1995; 34(6):878–887. [PubMed: 8598815]
19. Kim SG, Tsekos NV. Perfusion imaging by a flow-sensitive alternating inversion recovery (FAIR) technique: application to functional brain imaging. Magn Reson Med. 1997; 37(3):425–435. [PubMed: 9055234]
20. Detre JA, Alsop DC. Perfusion magnetic resonance imaging with continuous arterial spin labeling: methods and clinical applications in the central nervous system. Eur J Radiol. 1999; 30(2):115–124. [PubMed: 10401592]
21. Wong EC. Vessel-encoded arterial spin-labeling using pseudocontinuous tagging. Magn Reson Med. 2007; 58(6):1086–1091. [PubMed: 17969084]
22. Wu WC, Fernandez-Seara M, Detre JA, Wehrli FW, Wang J. A theoretical and experimental investigation of the tagging efficiency of pseudocontinuous arterial spin labeling. Magn Reson Med. 2007; 58(5):1020–1027. [PubMed: 17969096]

23. Duhamel G, Prevost V, Girard OM, Callot V, Cozzone PJ. High-resolution mouse kidney perfusion imaging by pseudo-continuous arterial spin labeling at 11.75T. Magn Reson Med. 2013
24. Pell GS, Lewis DP, Ordidge RJ, Branch CA. TurboFLASH FAIR imaging with optimized inversion and imaging profiles. Magn Reson Med. 2004; 51(1):46–54. [PubMed: 14705044]
25. Zuo Z, Wang R, Zhuo Y, Xue R, St Lawrence KS, Wang DJ. Turbo-FLASH based arterial spin labeled perfusion MRI at 7 T. PLoS One. 2013; 8(6):e66612. [PubMed: 23818950]
26. Wang J, Li L, Roc AC, Alsop DC, Tang K, Butler NS, Schnall MD, Detre JA. Reduced susceptibility effects in perfusion fMRI with single-shot spin-echo EPI acquisitions at 1.5 Tesla. Magn Reson Imaging. 2004; 22(1):1–7. [PubMed: 14972387]
27. Rajendran R, Lew SK, Yong CX, Tan J, Wang DJ, Chuang KH. Quantitative mouse renal perfusion using arterial spin labeling. NMR Biomed. 2013; 26(10):1225–1232. [PubMed: 23592238]
28. Esparza-Coss E, Wosik J, Narayana PA. Perfusion in rat brain at 7 T with arterial spin labeling using FAIR-TrueFISP and QUIPSS. Magn Reson Imaging. 2010; 28(4):607–612. [PubMed: 20299174]
29. Boss A, Martirosian P, Claussen CD, Schick F. Quantitative ASL muscle perfusion imaging using a FAIR-TrueFISP technique at 3.0 T. NMR Biomed. 2006; 19(1):125–132. [PubMed: 16404727]
30. Petersen ET, Zimine I, Ho YC, Golay X. Non-invasive measurement of perfusion: a critical review of arterial spin labelling techniques. Br J Radiol. 2006; 79(944):688–701. [PubMed: 16861326]
31. Yongbi MN, Yang Y, Frank JA, Duyn JH. Multislice perfusion imaging in human brain using the C-FOCI inversion pulse: comparison with hyperbolic secant. Magn Reson Med. 1999; 42(6): 1098–1105. [PubMed: 10571931]
32. Lu L, Erokwu B, Lee G, Gulani V, Griswold MA, Dell KM, Flask CA. Diffusion-prepared fast imaging with steady-state free precession (DP-FISP): a rapid diffusion MRI technique at 7 T. Magn Reson Med. 2012; 68(3):868–873. [PubMed: 22139974]
33. Shah T, Lu L, Dell KM, Pagel MD, Griswold MA, Flask CA. CEST-FISP: a novel technique for rapid chemical exchange saturation transfer MRI at 7 T. Magn Reson Med. 2011; 65(2):432–437. [PubMed: 20939092]
34. Gunther M, Bock M, Schad LR. Arterial spin labeling in combination with a look-locker sampling strategy: inflow turbo-sampling EPI-FAIR (ITS-FAIR). Magn Reson Med. 2001; 46(5):974–984. [PubMed: 11675650]
35. Deichmann R, Haase A. Quantification of T_1 Values by Snapshot-Flash Nmr Imaging. Journal of Magnetic Resonance. 1992; 96(3):608–612.
36. Jakob PM, Hillenbrand CM, Wang T, Schultz G, Hahn D, Haase A. Rapid quantitative lung ^1H T_1 mapping. J Magn Reson Imaging. 2001; 14(6):795–799. [PubMed: 11747038]
37. Herscovitch P, Raichle ME. What is the correct value for the brain--blood partition coefficient for water? J Cereb Blood Flow Metab. 1985; 5(1):65–69. [PubMed: 3871783]
38. Schmid-Elsaesser R, Zausinger S, Hungerhuber E, Baethmann A, Reulen HJ. A critical reevaluation of the intraluminal thread model of focal cerebral ischemia: evidence of inadvertent premature reperfusion and subarachnoid hemorrhage in rats by laser-Doppler flowmetry. Stroke. 1998; 29(10):2162–2170. [PubMed: 9756599]
39. Harada H, Wang Y, Mishima Y, Uehara N, Makaya T, Kano T. A novel method of detecting rCBF with laser-Doppler flowmetry without cranial window through the skull for a MCAO rat model. Brain Res Brain Res Protoc. 2005; 14(3):165–170. [PubMed: 15795170]
40. Durukan A, Tatlisumak T. Ischemic stroke in mice and rats. Methods Mol Biol. 2009; 573:95–114. [PubMed: 19763924]
41. Muir ER, Shen Q, Duong TQ. Cerebral blood flow MRI in mice using the cardiac-spin-labeling technique. Magn Reson Med. 2008; 60(3):744–748. [PubMed: 18727091]
42. Kober F, Duhamel G, Cozzone PJ. Experimental comparison of four FAIR arterial spin labeling techniques for quantification of mouse cerebral blood flow at 4.7 T. NMR Biomed. 2008; 21(8): 781–792. [PubMed: 18384177]
43. Duhamel G, Callot V, Cozzone PJ, Kober F. Spinal cord blood flow measurement by arterial spin labeling. Magn Reson Med. 2008; 59(4):846–854. [PubMed: 18383283]

44. Vasanawala SS, Pauly JM, Nishimura DG. Linear combination steady-state free precession MRI. Magn Reson Med. 2000; 43(1):82–90. [PubMed: 10642734]

45. Cukur T, Lustig M, Nishimura DG. Multiple-profile homogeneous image combination: application to phase-cycled SSFP and multicoil imaging. Magn Reson Med. 2008; 60(3):732–738. [PubMed: 18727089]

46. Haacke EM, Wielopolski PA, Tkach JA, Modic MT. Steady-state free precession imaging in the presence of motion: application for improved visualization of the cerebrospinal fluid. Radiology. 1990; 175(2):545–552. [PubMed: 2326480]

47. Miles KA. Measurement of tissue perfusion by dynamic computed tomography. Br J Radiol. 1991; 64(761):409–412. [PubMed: 2036562]

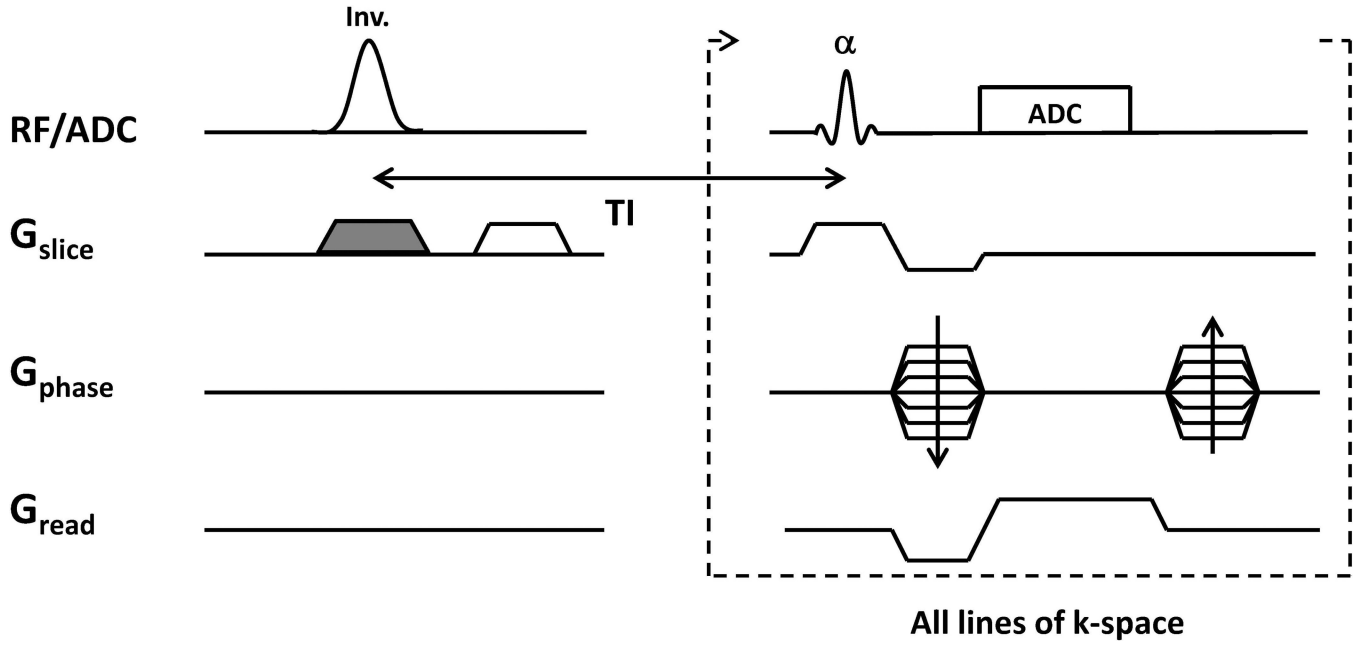

Figure 1.

Schematic of ASL-FISP acquisition. A FAIR ASL preparation is combined with a centrically-encoded FISP acquisition. This acquisition is repeated for both a slice-selective inversion (with shaded gradient) and a non-selective inversion (without the shaded gradient) to generate the perfusion contrast. Note that all lines of k-space are acquired following a single ASL preparation.

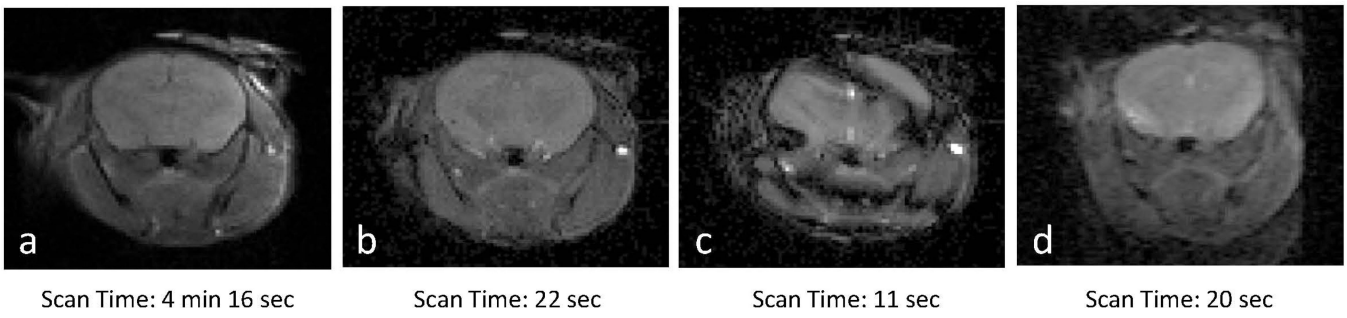

Figure 2.

Representative axial mouse brain images at 7 T using (a) spin echo, (b) FISP, (c) True FISP, and (d) EPI acquisitions. Note the similar lack of artifacts in the spin echo and FISP images in comparison to the True FISP (banding) and EPI (ghosting / distortion) images.

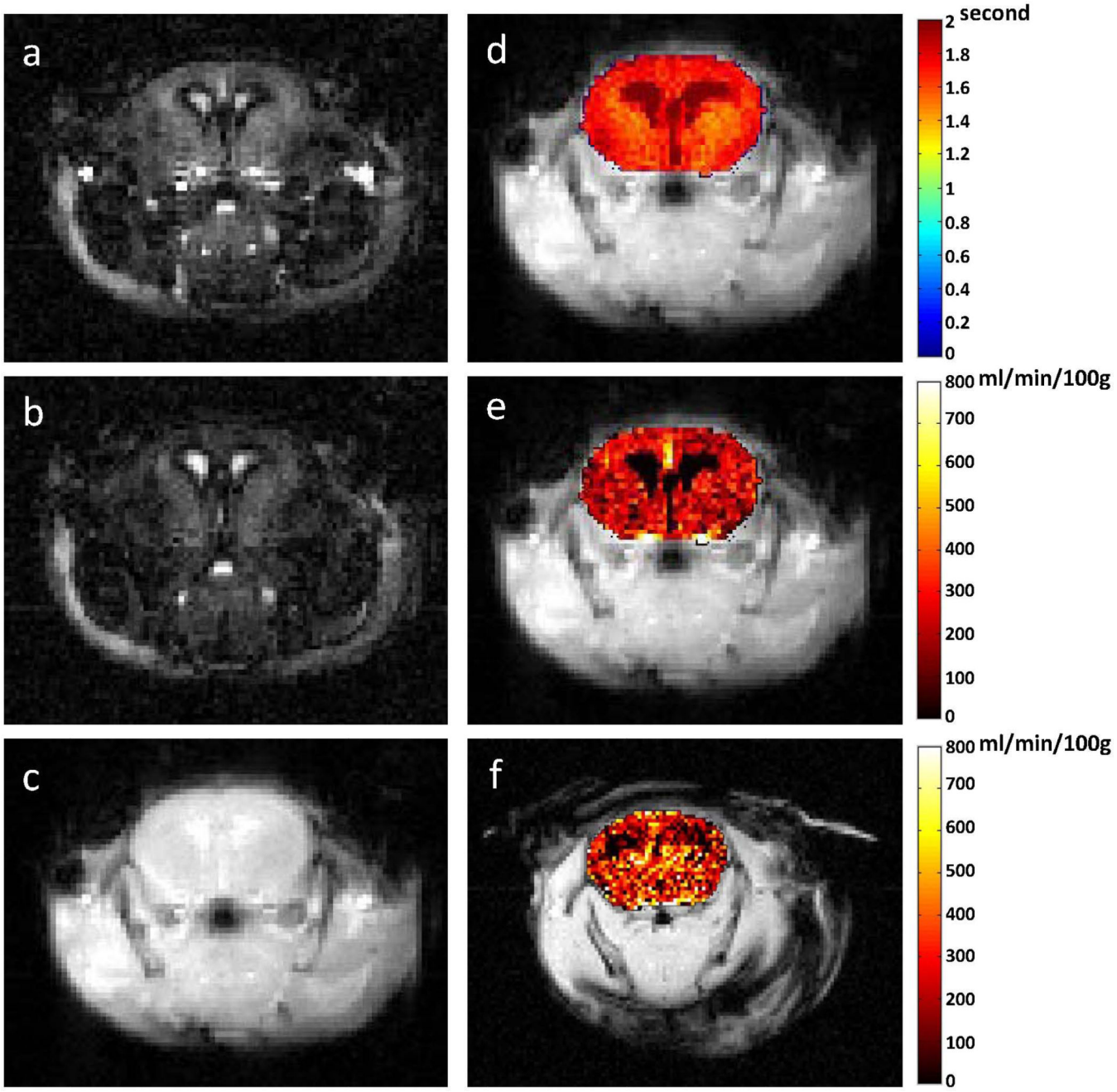

Figure 3.

Representative ASL-FISP images of a healthy C57/BL6 mouse brain at 7 T. (a) Slice-selective (bright-blood); (b) non-selective (dark blood) ASL-FISP images (40 averages); (c) M0 image (no inversion); (d) Brain T_1 map from Look-Locker acquisition; perfusion map from (e) ASL-FISP and (f) ASL-GRE in ml/min/100g of tissue. Note that the ASL-FISP and ASL-GRE perfusion maps are from different mice.

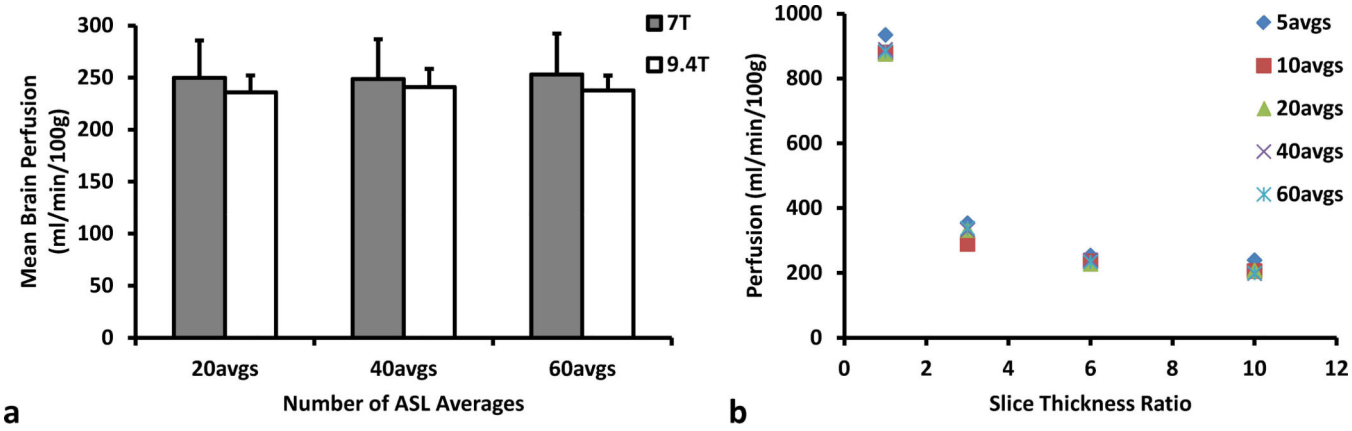

Figure 4.

(a) Mean C57/BL6 mouse brain perfusion from the ASL-FISP method at 7 T (gray) and 9.4 T (white), respectively. Results are plotted as a function of the number of ASL-FISP averages. No significant differences in mean perfusion were observed for different number of averages ($p > 0.6$) or field strength ($p > 0.2$). (b) Mean brain perfusion from a single C57/BL6 mouse at 7 T as a function of the slice thickness ratio (inversion slab thickness / imaging slice thickness) and the number of ASL-FISP averages. Note the large decrease in mean brain perfusion as the slice thickness ratio is increased from 1 to 3. The mean perfusion also appears to be more sensitive to the inversion slab thickness than the number of ASL-FISP averages.

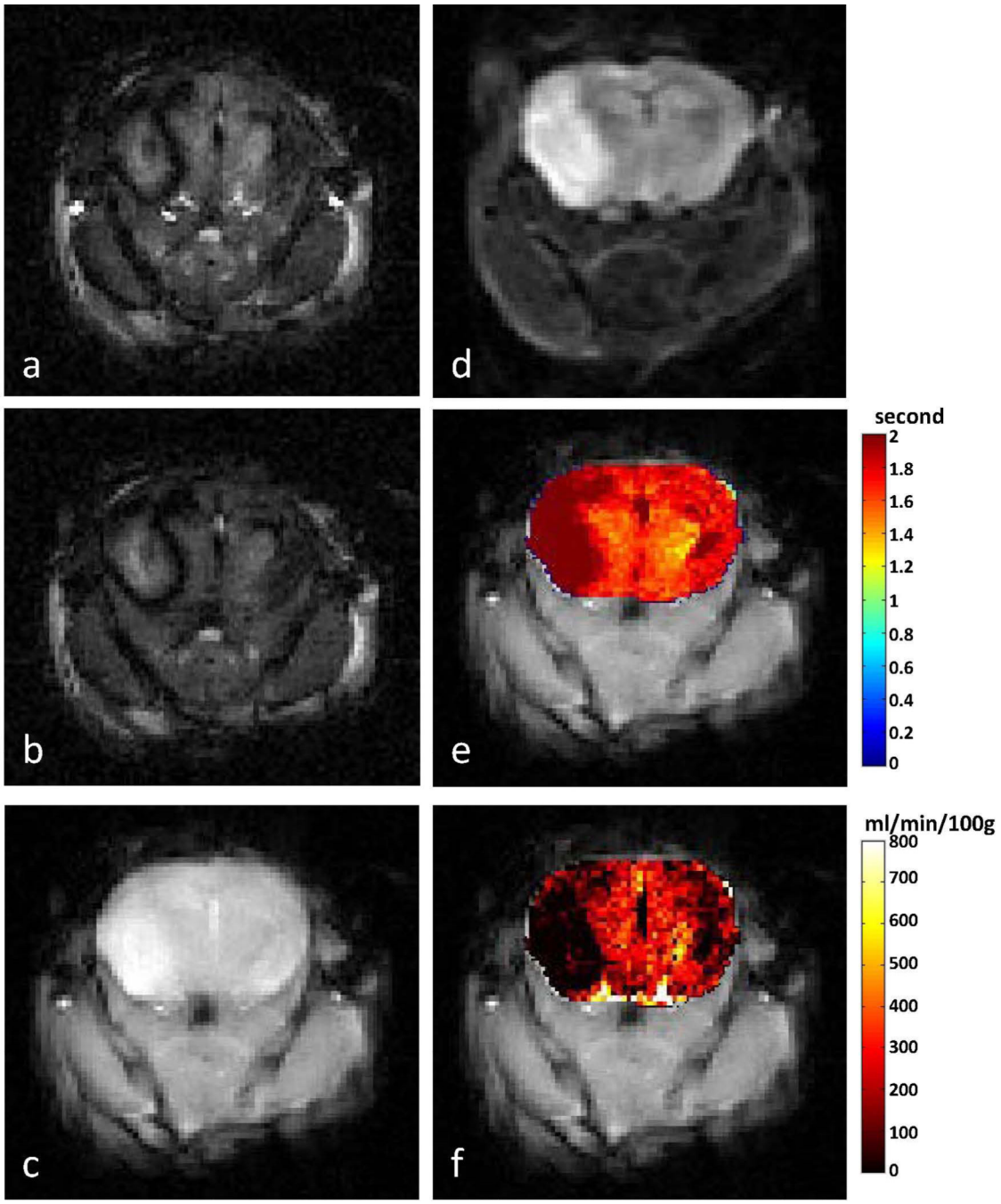

Figure 5.

ASL-FISP images of an MCAo mouse model of stroke at 7 T. (a) Slice-selective (bright-blood) and (b) non-selective (dark blood) ASL-FISP images; (c) M0 FISP image (no inversion); (d) diffusion-weighted image (b=500 s/mm^2) showing right brain infarct; (e) Look-Locker T_1 map; and (f) perfusion map. The primary infarct is visible in the right brain in all images. A potential contralateral perfusion deficit is also observed in the perfusion map, but less evident in T_1 and diffusion weighted images.

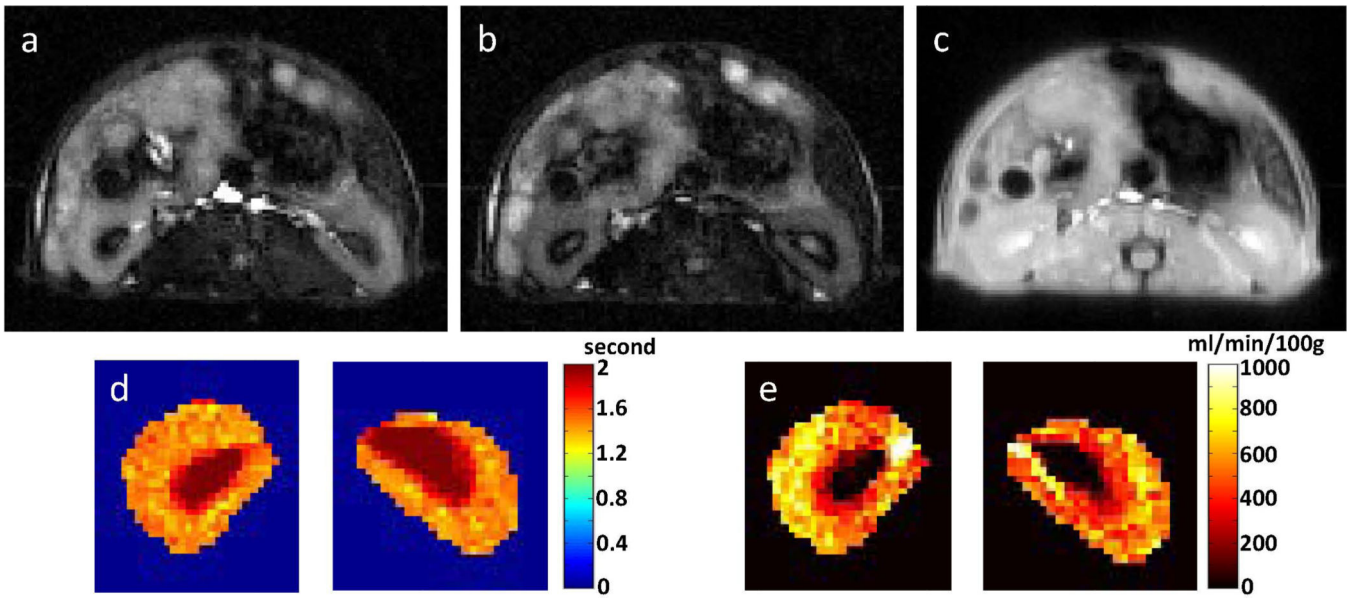

Figure 6.

Kidney ASL-FISP images from a healthy C57/BL6 mouse at 7 T. (a) Slice-selective (bright-blood) and (b) non-selective (dark blood) ASL-FISP images; (c) M0 FISP image (no inversion); (d) Look-Locker T_1 map; and (e) perfusion map. Renal arteries (high perfusion) and renal medulla (low perfusion) are clearly visible in the perfusion map.